

# Linear stability of radial displacements in porous media: Influence of velocity-induced dispersion and concentration-dependent diffusion

A. Riaz

*Department of Petroleum Engineering, Stanford University, Stanford, California 94305-2220*

C. Pankiewicz

*Lehrstuhl A für Thermodynamik, Technische Universität München, D-85747 Garching, Germany*

E. Meiburg<sup>a)</sup>

*Department of Mechanical and Environmental Engineering, University of California, Santa Barbara, Santa Barbara, California 93106-5070*

(Received 9 April 2004; accepted 2 June 2004; published online 13 August 2004)

A parametric study is conducted in order to investigate the influence of (a) velocity dependent dispersion, and (b) concentration-dependent diffusion on the stability of miscible porous media displacements in the radial geometry. Numerical solutions for the base concentration profile demonstrate that velocity induced dispersion dominates for short times and large Péclet numbers. For large times, the growth rates approach those obtained when only molecular diffusion is taken into account. Concentration-dependent diffusion coefficients are seen to modify the mobility profiles of the base flow, and to shift the eigenfunctions into more or less viscous environments. This results in a destabilization for nearly all Péclet values and mobility ratios. © 2004 American Institute of Physics. [DOI: 10.1063/1.1775431]

## I. INTRODUCTION

Past theoretical investigations have addressed many aspects of the linear stability problem arising when one fluid displaces another one of larger viscosity in a Hele–Shaw cell or porous medium. For the situation of miscible fluids in a radial source flow geometry, Tan and Homsy<sup>1</sup> employ a quasi-steady-state analysis, which shows that the unfavorable viscosity gradient results in an algebraically growing perturbation, rather than the exponential behavior known from rectilinear displacements. Pankiewicz and Meiburg<sup>2</sup> extend this analysis to fluid combinations giving rise to nonmonotonic viscosity profiles, which they find to be destabilizing. Riaz and Meiburg<sup>3</sup> report on the stability of axial and helical perturbations in three-dimensional displacements. Yortsos<sup>4</sup> incorporates the effects of equilibrium adsorption and shows the existence of a mathematical transformation that relates radial flows to rectilinear ones. A partial review, along with a discussion of the effects of heterogeneity, is provided by Yortsos.<sup>5</sup> Whenever the above studies account for molecular diffusion or mechanical dispersion, they do so by assuming a constant diffusion coefficient, which is found to have a stabilizing effect. However, the experimental measurements by Petitjeans and Maxworthy<sup>6</sup> demonstrate that this may not always be a good approximation. These authors find that, for example, the diffusion coefficient between water and glycerin varies by a factor of about 30, depending on the local concentration value. Hence an interesting question arises concerning the influence of this concentration dependence on the stability properties of miscible displacements. The dependence of the diffusivity on the concentration can be expected

to have two main effects. First of all, it will modify the concentration profile of the base flow. Second, it will affect the location of the perturbation eigenfunction within the base flow, as well as its shape and growth rate.

The issue of velocity induced dispersion has been addressed for rectilinear displacements by Yortsos and Zeybek<sup>7</sup> and by Zimmermann and Homsy.<sup>8</sup> The former authors compare the relative influence of molecular diffusion and velocity induced dispersion by means of a linear stability analysis. They show that displacements which take into account the velocity induced dispersion generally are more stable than those which account for molecular diffusion only. This is in line with expectation, as dispersion acts to spread out both the base profile as well as the perturbation itself. Since the dispersion coefficient in a realistic porous medium as well as in Hele–Shaw flows is commonly assumed to grow with increasing velocity, it should affect the radial flow problem in a qualitatively different way, as compared to the rectilinear problem. The base velocity in the latter is constant, leading to a uniformly stabilizing influence. On the other hand, the base velocity in radial flows decreases as  $1/r$  away from the source, so that the influence of dispersion can be expected to weaken over time. Thus there is a possibility that the level of instability can be higher at later times when the velocity induced dispersion cannot provide an appreciable stabilization.

Quantitative estimates regarding the different flow regimes can be obtained on the basis of classical Taylor dispersion results (Taylor<sup>9</sup>), which were modified for two-dimensional gaps by Horne and Rodriguez.<sup>10</sup> These authors show that the Taylor dispersion coefficient can be quantified as  $\frac{2}{945}(d^2U^2/D')$ , where  $d$  is the gap width,  $U$  denotes the centerline velocity, and  $D'$  indicates the molecular diffusion

<sup>a)</sup>Author to whom correspondence should be addressed. Electronic mail: meiburg@engineering.ucsb.edu

coefficient. For a typical “lab-on-a-chip” application, one may assume  $D=O(10^{-6} \text{ cm}^2/\text{s})$  and  $d=O(10 \text{ }\mu\text{m})$ . For  $U=O(1 \text{ mm/s})$ , Taylor dispersion dominates, whereas for  $U=O(100 \text{ }\mu\text{m/s})$ , molecular diffusion can be expected to outweigh dispersion. These rough estimates demonstrate that both of these regimes may be attained in microfluidic applications, cf. also the recent review article by Stone *et al.*<sup>11</sup>

Petitjeans *et al.*<sup>12</sup> carry out both experiments as well as numerical simulations in order to gain insight into the role of mechanical dispersion in variable viscosity, radial Hele–Shaw displacements. They observe that numerical simulations employing a Taylor dispersion model are unable to accurately reproduce the experimental data. Most likely, this is due to the fact that Taylor’s model is based on the assumption of Poiseuille flow, which does not exist in the presence of significant viscosity gradients. For this reason, here we model dispersion in radial flows based on the model proposed by Bear.<sup>13</sup> The outline of this paper is as follows: Section II states the set of governing equations and derives the eigenvalue problem. Section III begins by discussing the effects of velocity induced dispersion on the base concentration profile, as well as on the dispersion relations. Subsequently, the role of concentration-dependent diffusivities is addressed as a function of the Péclet number, and related scaling behaviors are identified. Section IV summarizes the main findings and conclusions from this investigation.

## II. GOVERNING EQUATIONS

We consider the problem of radial source flow in a homogeneous porous medium of constant permeability. Fluid 1 is injected at a constant flow rate  $Q$ , thereby displacing fluid 2. The fluids are assumed to be miscible in all proportions, with a molecular diffusion coefficient  $D'(c)$  that depends on the concentration  $c$  of the solvent, which is taken to be unity in the displaced fluid. We assume a linear relationship for  $D'(c)$  of the form

$$D(c) = \frac{D'(c)}{\bar{D}} = \frac{2}{S+1} + 2\frac{S-1}{S+1}c \quad \text{with} \quad S = \frac{D'(c=1)}{D'(c=0)}, \tag{1}$$

where

$$\bar{D} = \int_0^1 D'(c)dc. \tag{2}$$

The above linear dependence closely tracks real fluid combinations such as water and glycerin, cf. Petitjeans and Maxworthy.<sup>6</sup> For most fluids,  $D'$  decreases with increasing viscosity (cf. Bird, Stewart, and Lightfoot<sup>14</sup>), which suggests values  $S < 1$ . However, for the sake of completeness we will consider values of  $S$  both smaller and larger than unity.

The analysis to be presented in the following closely follows earlier work by Tan and Homsy<sup>1</sup> and by our own group.<sup>2,3</sup> However, all of these earlier investigations addressed situations with constant diffusion coefficients and in the absence of flow induced dispersion. By employing Darcy’s law, one arrives at the dimensionless equations in cylindrical coordinates,

$$\nabla \cdot \mathbf{u} = 0, \tag{3}$$

$$\mathbf{u} = -\mu \nabla p, \tag{4}$$

$$\frac{\partial c}{\partial t} + \mathbf{u} \cdot \nabla c = \nabla \cdot \mathbf{D} \cdot \nabla c. \tag{5}$$

Here  $\mu$  indicates the viscosity, which has been rendered dimensionless by the lower viscosity of the displacing fluid. In line with earlier authors, the functional relationship between viscosity and concentration is taken to be

$$\mu = e^{Rc}. \tag{6}$$

The dispersion tensor  $\mathbf{D}$  can be expressed as<sup>15–18</sup>

$$\mathbf{D} = \left( \beta|\mathbf{u}| + \frac{1}{Pe}D \right) \mathbf{I} + \gamma\beta \frac{\mathbf{u}\mathbf{u}}{|\mathbf{u}|}, \tag{7}$$

where the Péclet number  $Pe$  is defined as

$$Pe = \frac{Q}{\bar{D}} \tag{8}$$

and

$$\beta = \frac{\alpha_T}{L}, \tag{9}$$

$$\gamma = \frac{\alpha_L}{\alpha_T} - 1. \tag{10}$$

The longitudinal and transverse dispersivities (units of length) are  $\alpha_L$  and  $\alpha_T$ , respectively, while  $L$  indicates a macroscopic length scale, such as the radius of the nominally axisymmetric front.<sup>3</sup>  $\mathbf{I}$  denotes the unit diagonal matrix. Gelhar *et al.*<sup>18</sup> present careful experimental studies to determine the magnitude of  $\alpha_L$  and  $\alpha_T$ . Although strictly valid only for tracer flows, we use their analysis and employ values of  $\beta = 10^{-4}$  and  $\alpha_T = 0.1 \alpha_L$ . Their work furthermore suggests that for variable viscosity displacements the value of  $\beta$  can be even smaller than  $10^{-4}$ .

The above equations allow for the axisymmetric base state velocity profile  $u_0 = 1/r$  and  $v_0 = 0$ . Since the problem does not contain an external length scale, we transform the equations to the new variable  $\eta = r\sqrt{Pe/2t}$ , for which the equation governing the base state concentration  $c_0$  becomes

$$2t \frac{\partial c_0}{\partial t} = \left\{ D_0 + \frac{Pe^{3/2}\beta}{\eta\sqrt{2t}}(1+\gamma) \right\} \frac{\partial^2 c_0}{\partial \eta^2} + \left\{ (D_0 - Pe) \frac{1}{\eta} + \eta + \frac{\partial D_0}{\partial \eta} \right\} \frac{\partial c_0}{\partial \eta}, \tag{11}$$

where  $D_0 = D(c_0)$ .

The linearized stability equations are obtained by expressing the dependent variables as a sum of base and perturbation components. The perturbation variables are then decomposed into normal modes whose amplitude depends on  $\eta$ ,

$$(u, c)(r, \theta, t) = \left( \frac{\hat{u}}{\eta}, \hat{c} \right) (\eta) f(t) e^{in\theta}. \tag{12}$$

We thus obtain the system of equations,

$$\frac{d^2 \hat{u}}{d\eta^2} + \left( \frac{1}{\eta} + Rc'_0 \right) \frac{d\hat{u}}{d\eta} - \frac{n^2}{\eta} \hat{u} - R \frac{n^2}{\eta} \hat{c} = 0, \tag{13}$$

$$\begin{aligned} & \left\{ D_{m_0} + \frac{\beta Pe^{3/2}}{\eta \sqrt{2t}} (1 + \gamma) \right\} \frac{d^2 \hat{c}}{d\eta^2} + \left\{ \frac{1}{\eta} (D_{m_0} - Pe) \right. \\ & + 4 \frac{S-1}{S+1} c'_0 \left. \right\} \frac{d\hat{c}}{d\eta} + \left\{ 2 \frac{S-1}{S+1} \left( \frac{1}{\eta} c'_0 + c''_0 \right) \right. \\ & + \frac{n^2}{\eta^2} \left( D_{m_0} + \frac{\beta Pe^{3/2}}{\eta \sqrt{2t}} \right) \left. \right\} \hat{c} + \frac{\beta Pe^{3/2}}{\eta \sqrt{2t}} c'_0 \frac{d\hat{u}}{d\eta} \\ & + \left\{ \frac{\beta Pe^{3/2}}{\eta \sqrt{2t}} (1 + \gamma) c''_0 - \frac{Pe}{\eta} c'_0 \right\} \hat{u} = \sigma \hat{c}, \end{aligned} \tag{14}$$

where primes denote derivatives with respect to  $\eta$ . The above equations define an eigenvalue problem with an algebraic eigenvalue  $\sigma$  given by

$$\sigma = 2t \frac{1}{f} \frac{df}{dt} \tag{15}$$

for the boundary conditions  $(\hat{u}, \hat{c}) \rightarrow 0$  with  $\eta \rightarrow 0$  and  $\eta \rightarrow \infty$ . The growth rate of a given mode with wave number  $n$  is seen to depend on  $Pe$ ,  $R$ ,  $S$  and the properties of the relationships  $\mu(c)$  and  $D(c)$ . The stability equations (13) and (14) have to be solved numerically to obtain the dispersion relations. Toward this end, we employ a finite difference approximation to the equations that transforms the differential eigenvalue problem into a general algebraic eigenvalue problem which can then be solved applying standard methods.<sup>2,3</sup>

### III. RESULTS

#### A. Influence of dispersion

We first analyze the influence of the velocity-induced dispersion ( $\beta \neq 0$ ) using a constant diffusion coefficient  $S = 1$ . Figure 1(a) presents the concentration base profile as obtained by solving Eq. (11) for different times and  $Pe = 100$ . Initially the  $\beta \neq 0$  profiles are less steep than the  $\beta = 0$  profile. However, they approach the latter for large times, reflecting the diminishing importance of dispersion. The increased gradients of the base state for late times result in higher growth rates, which approach those of the case without dispersion, as shown in Fig. 1(b). These dispersion relations are obtained by solving Eqs. (13) and (14).

The effect of increasing the Péclet number is shown in Fig. 2, which presents results for  $Pe = 1000$ . For this case, the base profiles in the presence of dispersion are considerably less steep than the  $\beta = 0$  profile, even at large times. Consequently, the growth rates are significantly smaller as compared to the  $\beta = 0$  case, as shown in Fig. 2(b). This observation indicates that the influence of velocity induced dispersion is more important for larger Péclet numbers, in line with expectation.

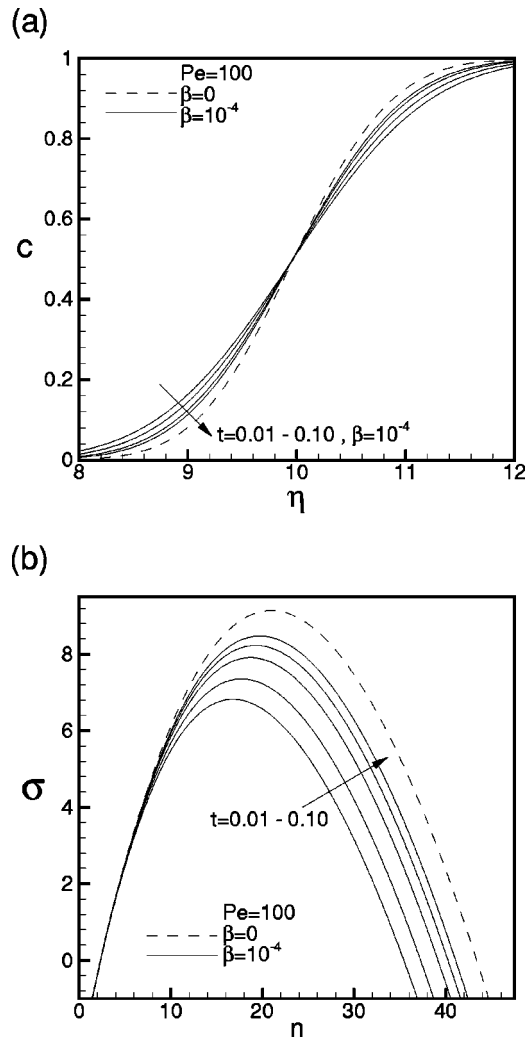


FIG. 1. Influence of velocity induced dispersion. (a) Base concentration profiles for  $Pe=100$  and  $\beta=10^{-4}$  at different times (solid lines), and for  $\beta = 0$  (dashed line). The base state in the presence of velocity induced dispersion asymptotically approaches the base state without dispersion. (b) Dispersion relations for  $Pe=100$ ,  $R=5$ , and  $\beta=10^{-4}$  at different times (solid lines), and for  $\beta=0$  (dashed line). The growth rates for the case with dispersion asymptotically approach the values for the case without dispersion.

#### B. Influence of variable diffusion

In the following, we investigate the effect of variable diffusion coefficients, as given by Eq. (1), on the stability properties of the radial displacement. During this analysis, the dispersion coefficient  $\beta$  is set to zero, which effectively limits the applicability to late times.

Figure 3(a) compares numerically computed base states for  $Pe=400$  and variable diffusion coefficients with the analytic solution for a constant diffusion coefficient displacement at the same value of  $Pe$  (cf. Tan and Homsy<sup>1</sup>). The location of the “mean” interface, defined by  $c=0.5$ , depends weakly on  $S$  and is given approximately by  $\eta = Pe^{1/2}$  for all values of  $S$ . Since  $D$  reaches its extrema for  $c=0$  and 1, the variable diffusion coefficient predominantly influences the tails of the concentration profile. Hence, while the slope of the concentration profile does not vary strongly with  $S$  near the mean position of the interface, it becomes considerably steeper on the side with the lower diffusion coefficient, and

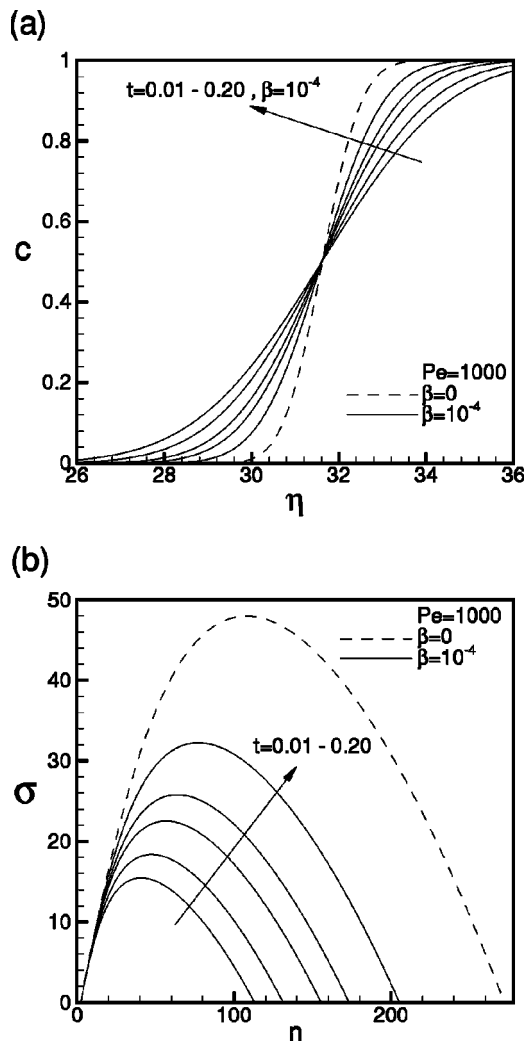


FIG. 2. Influence of velocity induced dispersion. (a) Base concentration profiles for  $Pe=1000$  and  $\beta=10^{-4}$  at different times (solid lines), and for  $\beta=0$  (dashed line). (b) Dispersion relations for  $Pe=100$ ,  $R=5$ , and  $\beta=10^{-4}$  at different times (solid lines), and for  $\beta=0$  (dashed line). The base states and dispersion relations are qualitatively similar to the smaller  $Pe$  case shown in Fig. 1. However, the difference between the cases with and without dispersion is greater even for large times, indicating a dominance of dispersion over diffusion for higher Péclet numbers.

correspondingly more gentle on the opposite side. Due to the exponential dependence of the viscosity on concentration differences among the viscosity profiles for various  $S$  values are more pronounced near  $c=1$ , cf. Fig. 3(b).

In order to investigate the stability properties of the displacement, the growth rate vs wave number dispersion relations are numerically determined from Eqs. (13) and (14) for various values of  $Pe$ ,  $R$ , and  $S$ . Typical results for different values of  $S$  with  $Pe=400$  and  $R=5$  are shown in Fig. 4. It can be observed that the maximum rate of growth increases both for  $S>1$  and for  $S<1$ . Both the most dangerous wave number and the cutoff wave number shift to larger values. For  $S>1$ , the maximum growth rate for the  $1/S$  case is slightly smaller than that for the corresponding  $S$  case, while the cutoff wave number is larger for the  $1/S$  case. The reason for this will become clear later, when we examine the eigen-

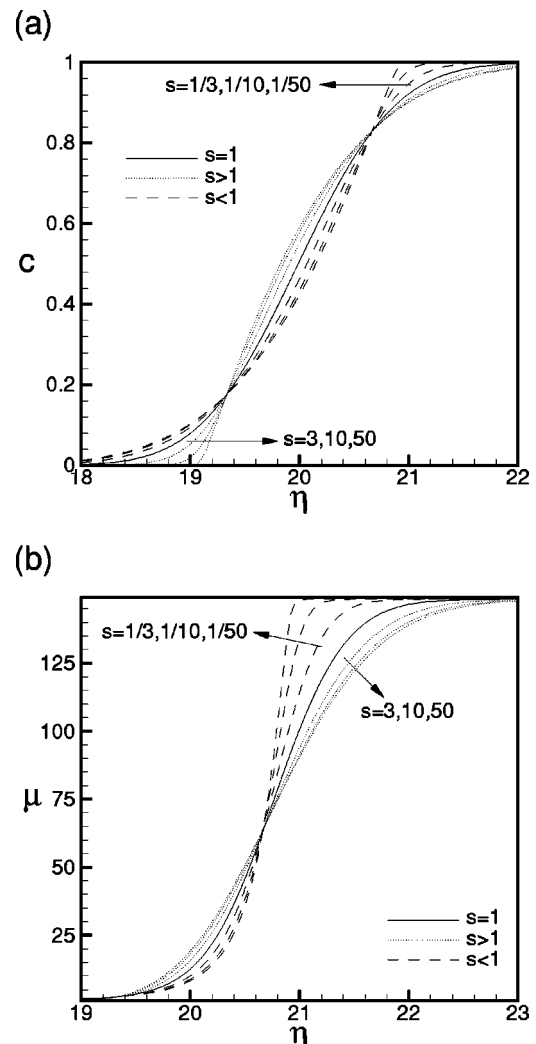


FIG. 3. Influence of concentration dependent diffusion on (a) the concentration base state and (b) the viscosity base profile, for  $Pe=400$ ,  $R=2.5$  and various values of  $S$ . Depending upon  $S$ , the concentration gradient becomes steeper on one end and more gentle on the other end, as compared to the constant diffusion coefficient profile. On the other hand, the viscosity profile becomes uniformly steeper over much of the interfacial region for values  $S<1$ .

functions below. For values of  $S$  near 50, the increase in the maximum growth rate is seen to be about 30%.

Figure 5 shows the maximum growth rate for  $S$  and  $1/S$  as function of  $Pe$  [Fig. 5(a)] and  $R$  [Fig. 5(b)], respectively. It is shown to increase from the  $S=1$  case for both  $S>1$  and  $S<1$ , for all values of  $Pe$  and  $R$ . Figure 6(a) displays  $\sigma_{max}$  values for  $R=5$ , as function of  $S$ , with  $Pe$  as a parameter. The growth rate generally increases with  $Pe$ . In addition, the figure suggests that both low and high values of  $S$  have a destabilizing effect on the displacement, with the growth rate reaching a minimum around  $S \approx 1$ .

In order to explore the governing scaling behavior in the presence of a variable diffusion coefficient, the growth rates presented in Fig. 6(a) are normalized by their corresponding values at  $S=1$ . The resulting curves, shown in Fig. 6(b), are seen to collapse for  $S<1$ . For  $S>1$ , on the other hand, the

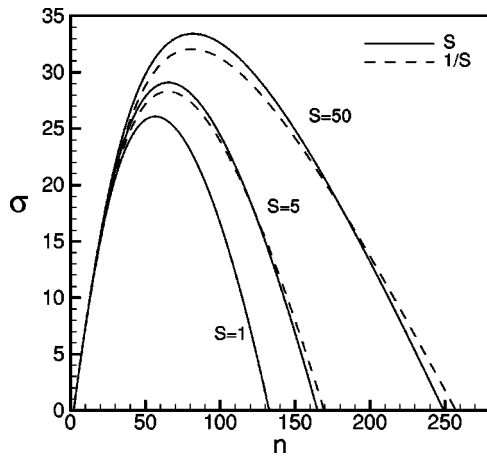


FIG. 4. Influence of the variable diffusion coefficient on the dispersion relation for  $Pe=400$  and  $R=5$ . Both  $S>1$  and  $S<1$  lead to increasing growth rates, maximum and cutoff wave numbers.

collapse is less complete as  $S$  becomes very large. This behavior is also evident at a smaller viscosity ratio  $R=3$ , as shown in Fig. 6(c).

Close inspection shows that for  $S$  near to but less than one, variable diffusion coefficients can have a slightly stabilizing influence on the displacement. This effect is more

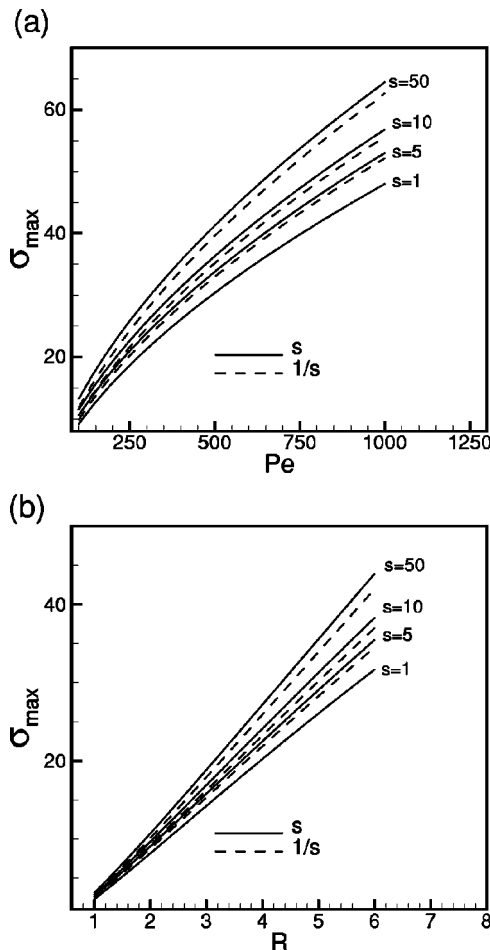


FIG. 5. Growth rates of the most unstable mode as a function of (a)  $Pe$ , and (b)  $R$  for various values of  $S$ .  $S \neq 1$  is seen to be destabilizing across the entire range of  $Pe$  and  $R$  shown.

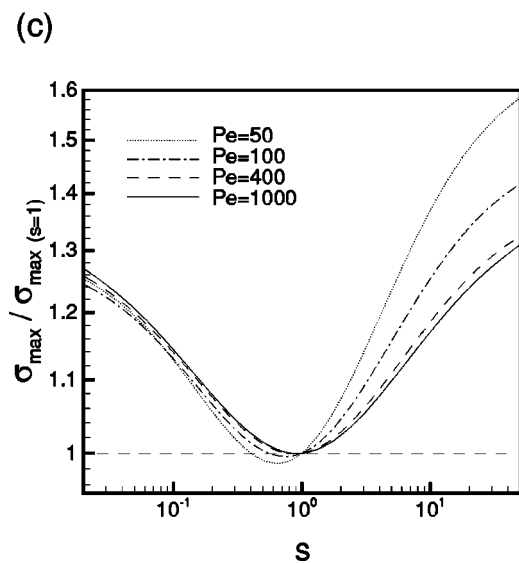
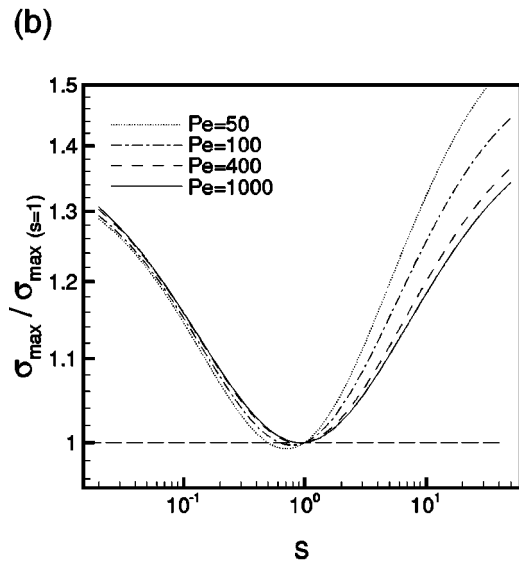
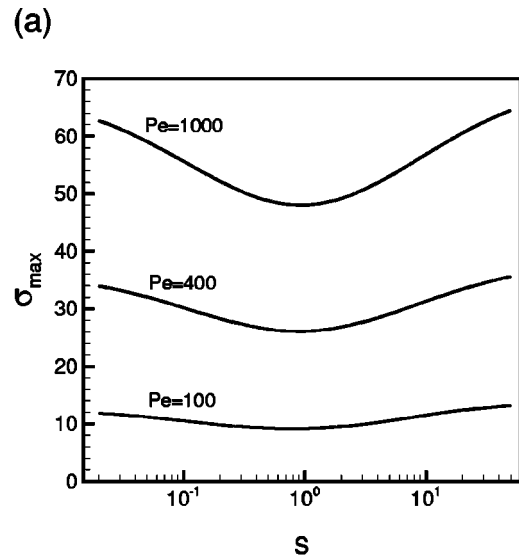


FIG. 6. (a) The maximum growth rate as a function of  $S$  for various values of  $Pe$  and  $R=5$ . (b) The maximum growth rate of (a), normalized by the maximum growth rate for the  $S=1$  case. (c) Normalized maximum growth rate for different values of  $Pe$  and  $R=3$ . The normalized curves in (b) and (c) are seen to collapse for  $S<1$ .



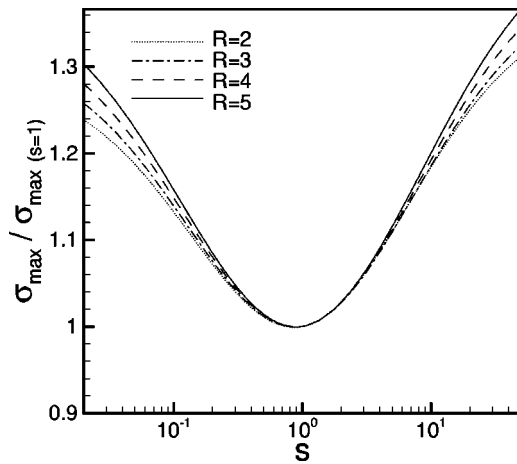


FIG. 7. Normalized maximum rate of growth as a function of  $S$  for different values of  $R$  and  $Pe=400$ . These curves collapse for both  $S > 1$  and  $S < 1$  in the neighborhood  $S \approx 1$ .

prominent and extends to lower values of  $S$  for small  $Pe$  values. Below a certain  $S=S^* < 1$  and for  $S > 1$ , the growth rate exceeds that of the corresponding constant diffusion coefficient displacement. For  $S > 1$ , lower Péclet numbers result in a stronger increase of  $\sigma_{\max}/\sigma_{\max}(S=1)$ . Additionally, the growth rates generally are higher for values of  $S > 1$ , as compared to the corresponding value at the “inverse” location  $1/S$ . Visual inspection of the results suggests that for  $Pe \rightarrow \infty$  an asymptotic curve for  $\sigma_{\max}/\sigma_{\max}(S=1)$  will be reached that depends only on the mobility ratio  $R$ . This is confirmed by Fig. 7, which shows the normalized curves to collapse for both  $S > 1$  and  $S < 1$  in the neighborhood of  $S \approx 1$ . Therefore, in the limit  $Pe \rightarrow \infty$ , for a given mobility ratio the dependence of the maximum growth rate  $\sigma_{\max}$  on the two-dimensional parameter space spanned by  $Pe$  and  $S$  can be reduced to the two one-dimensional relations  $\sigma_{\max}(S=1) = f(Pe)$  and  $\sigma_{\max}/\sigma_{\max}(S=1) = f(S)$ . We remark that this finding holds not only for the maximum growth rate, but also for the wave number of the most dangerous mode, so that the relation  $n_{\max} = f(Pe, S)$  can be replaced by the two one-dimensional functions  $n_{\max}(S=1) = f(Pe)$  and  $n_{\max}/n_{\max}(S=1) = f(S)$ .

In the following, we will attempt to explain the above results from a physical point of view. The overall reason for the instability is the existence of an unfavorable mobility profile in the flow. From earlier investigations of the constant diffusion coefficient case (e.g., Tan and Homay<sup>1</sup>), it is well known that the growth rate of the instability increases with the Péclet number, i.e., with an increasingly steep viscosity profile. Figure 3(b) shows that for constant  $Pe$  and  $S$  values significantly smaller than one, the viscosity profiles become steeper over much of the front, which explains the larger growth rates for this  $S$  regime.

For  $S > 1$ , the reason for the destabilization is not quite so obvious, since now the viscosity profile is less steep over much of the front, cf. Fig. 3(b). Here it helps to inspect the eigenfunctions more closely. Figure 8 depicts the velocity eigenfunctions for the  $S$  values of 1, 0.1, and 10. The  $S = 0.1$  eigenfunction is shifted towards larger radii, where the

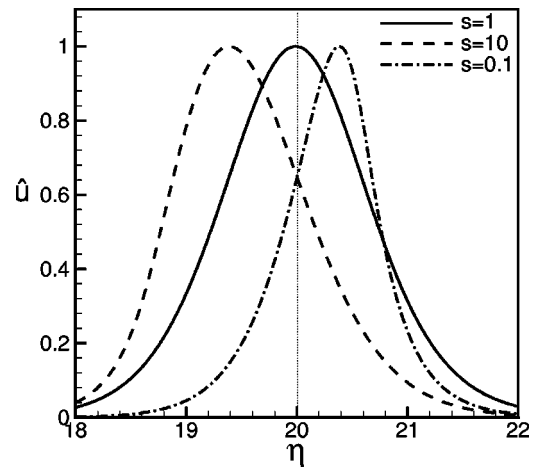


FIG. 8. The velocity eigenfunctions associated with the maximum growth rate for different values of  $S$ . The mean interface position  $c=0.5$  is shown in dotted line. The eigenfunction shifts inwards towards smaller  $c$  and lower viscosities values for  $S > 1$ , and it shifts slightly outwards towards higher  $c$  and larger viscosities values for  $S < 1$ .

concentration gradient is steeper (Fig. 3). For  $S=10$ , on the other hand, the eigenfunction is shifted inwards. We note that this radially inward shift represents a shift into a less viscous environment, which in turn facilitates more rapid growth. The weak stabilization observed for  $S$  values slightly smaller than unity can then be explained by the competing consequences of a radially outward shift, viz. a locally steeper concentration profile and a local increase in the viscosity.

#### IV. CONCLUSIONS

A linear stability analysis of radial, miscible displacements in porous media and Hele–Shaw flows has been carried out, in order to gain insight into the roles played by velocity induced dispersion and concentration-dependent diffusion coefficients. The results show that, as expected, dispersion tends to dominate over diffusion for large values of the Péclet number. However, due to the radially decreasing velocity values, the importance of dispersion decreases with time, so that the growth rates asymptotically approach those obtained when only molecular diffusion is taken into account.

Concentration dependent diffusion coefficients are seen to affect the stability problem in competing ways: They modify the mobility profiles of the base flow, rendering them locally steeper or gentler, and they lead to a radial shift of the eigenfunctions into more or less viscous environments. Overall, concentration dependent diffusion is seen to be destabilizing for nearly all Péclet values and mobility ratios. However, for small Péclet numbers and values of  $S$  slightly below unity a slight stabilization is observed. Maximum growth rates as well as the corresponding wave numbers tend to increase significantly for both small and large values of  $S$ . When normalized by their values for  $S=1$ , the maximum growth rates for different  $Pe$  values are seen to collapse for  $S < 1$ .

## ACKNOWLEDGMENTS

This research has been supported by the donors of The Petroleum Research Fund, administered by the American Chemical Society (Grant ACS-PRF No. 33497-AC9), by the University of California Energy Institute, and by the Chevron Petroleum Technology Company.

- <sup>1</sup>C. T. Tan and G. M. Homsy, "Stability of miscible displacements in porous media: Radial source flow," *Phys. Fluids* **30**, 1239 (1987).
- <sup>2</sup>C. Pankiewitz and E. Meiburg, "Miscible porous media displacements in the quarter five-spot configuration. Part 3. Non-monotonic viscosity profiles," *J. Fluid Mech.* **388**, 171 (1999).
- <sup>3</sup>A. Riaz and E. Meiburg, "Radial source flows in porous media: Linear stability analysis of axial and helical perturbations in miscible displacements," *Phys. Fluids* **15**, 938 (2003).
- <sup>4</sup>Y. C. Yortsos, "Stability of displacement processes in porous media in radial flow geometries," *Phys. Fluids* **30**, 2928 (1987).
- <sup>5</sup>Y. C. Yortsos, "Instabilities in displacement processes in porous media," *J. Phys.: Condens. Matter* **2**, SA443 (1990).
- <sup>6</sup>P. Petitjeans and T. Maxworthy, "Miscible displacements in capillary tubes. Part 1. Experiments," *J. Fluid Mech.* **326**, 37 (1996).
- <sup>7</sup>Y. C. Yortsos and M. Zeybek, "Dispersion driven instability in miscible displacements in porous media," *Phys. Fluids* **31**, 3511 (1988).
- <sup>8</sup>W. B. Zimmerman and G. M. Homsy, "Nonlinear viscous fingering in miscible displacement with anisotropic dispersion," *Phys. Fluids A* **3**, 1859 (1991).
- <sup>9</sup>G. I. Taylor, "Dispersion of soluble matter in solvent flowing slowly through a tube," *Proc. R. Soc. London, Ser. A* **124**, 186 (1953).
- <sup>10</sup>R. N. Horne and F. Rodriguez, "Dispersion in tracer flow in fractured geothermal systems," *Geophys. Res. Lett.* **10**, 289 (1983).
- <sup>11</sup>H. A. Stone, A. D. Stroock, and A. Ajdari, "Engineering flows in small devices," *Annu. Rev. Fluid Mech.* **36**, 381 (2004).
- <sup>12</sup>P. Petitjeans, C.-Y. Chen, E. Meiburg, and T. Maxworthy, "Miscible quarter five-spot displacements in a Hele-Shaw cell and the role of flow-induced dispersion," *Phys. Fluids* **11**, 1705 (1999).
- <sup>13</sup>J. Bear, *Dynamics of Fluids in Porous Media* (Wiley, New York, 1972).
- <sup>14</sup>R. Bird, W. Stewart, and E. N. Lightfoot, *Transport Phenomena* (Wiley, New York, 1966).
- <sup>15</sup>L. W. Gelhar and C. L. Axness, "Three-dimensional stochastic analysis of macrodispersion in aquifers," *Water Resour. Res.* **19**, 161 (1983).
- <sup>16</sup>D. J. Goode and L. F. Konikow, "Apparent dispersion in transient ground water flow," *Water Resour. Res.* **26**, 2339 (1990).
- <sup>17</sup>H. A. Tchelepi, F. M. Orr, Jr., N. Rakotomalala, D. Salin, and R. Woumeni, "Dispersion, permeability heterogeneity and viscous fingering: Acoustic experimental observations and particle tracking simulations," *Phys. Fluids A* **5**, 1558 (1993).
- <sup>18</sup>L. W. Gelhar, C. Welty, and K. R. Rehfeldt, "A critical review of data on field-scale dispersion in aquifers," *Water Resour. Res.* **28**, 1955 (1992).